Conformational Changes in the Amino-Terminal Helix of the G Protein α_{i1} Following Dissociation From G$\beta\gamma$ Subunit and Activation

Martina Medkova,[§,⊥] Anita M. Preininger,[§,⊥] Nan-Jun Yu,[‡] Wayne L. Hubbell,[*,‡] and Heidi E. Hamm[*,§,||]

Department of Pharmacology, Vanderbilt University Medical Center, 23rd Avenue South @ Pierce, 442 Robinson Research Building, Nashville, Tennessee 37232-6600, Department of Molecular Pharmacology and Biological Chemistry, Institute for Neuroscience, Northwestern University, Chicago, Illinois 60611, and Departments of Ophthalmology and Chemistry, University of California at Los Angeles, California 90095

Received January 22, 2002; Revised Manuscript Received June 10, 2002

ABSTRACT: G protein α subunits mediate activation of signaling pathways through G protein-coupled receptors (GPCR) by virtue of GTP-dependent conformational rearrangements. It is known that regions of disorder in crystal structures can be indicative of conformational flexibility within a molecule, and there are several such regions in G protein α subunits. The amino-terminal 29 residues of Gα are α-helical only in the heterotrimer, where they contact the side of Gβ, but little is known about the conformation of this region in the active GTP bound state. To address the role of the Gα amino-terminus in G-protein activation and to investigate whether this region undergoes activation-dependent conformational changes, a site-directed cysteine mutagenesis study was carried out. Engineered $G\alpha_{i1}$ proteins were created by first removing six native reactive cysteines to yield a mutant $G\alpha_{i1}$−C3S−C66A−C214S−C305S−C325A−C351I that no longer reacts with cysteine-directed labels. Several cysteine substitutions along the amino-terminal region were then introduced. All mutant proteins were shown to be folded properly and functional. An environmentally sensitive probe, Lucifer yellow, linked to these sites showed a fluorescence change upon interaction with G$\beta\gamma$ and with activation by AlF_4^-. Other fluorescent probes of varying charge, size, and hydrophobicity linked to amino-terminal residues also revealed changes upon activation with bulkier probes reporting larger changes. Site-directed spin-labeling studies showed that the N-terminus of the Gα subunit is dynamically disordered in the GDP bound state, but adopts a structure consistent with an α-helix upon interaction with G$\beta\gamma$. Interaction of the resulting spin-labeled G$\alpha\beta\gamma$ with photoactivated rhodopsin, followed by rhodopsin-catalyzed GTPγS binding, caused the amino-terminal domain of Gα to revert to a dynamically disordered state similar to that of the GDP-bound form. Together these results suggest conformational changes occur in the amino-termini of $G\alpha_i$ proteins upon subunit dissociation and upon activating conformational changes. These solution studies reveal insights into conformational changes that occur dynamically in solution.

Heterotrimeric G proteins ($\alpha\beta\gamma$)[1] couple a variety of seven transmembrane receptors to appropriate effector proteins. Much of our mechanistic understanding of G-protein signaling comes from numerous structural studies. The crystal structures of heterotrimeric G_t (*1*) and G_i (*2*) have allowed the identification of subunit binding sites and provided a fundamental context for understanding how the G protein heterotrimer interacts with membranes and the activated receptor, and how GTP binding leads to subunit dissociation and effector activation. In both G_t and G_i heterotrimeric crystal structures, the amino-termini of Gα subunits are resolved as α-helices interacting with G$\beta\gamma$ (*1*, *2*). In the $G\alpha_i$-GDP crystal structure (*3*) the amino-terminus of $G\alpha_i$ is organized into a compact microdomain with the carboxyl terminus, but it is disordered in $G\alpha_i$-GTPγS (*4*). The reported crystal structures of $G\alpha_t$-GDP (*5*) and $G\alpha_t$-GTPγS (*6*) bound states both lack the first 25 residues. Since the amino- and carboxyl-terminal regions are not visible in crystal structures of the free Gα subunits, and since few details of amino-terminal conformation are available from these structures, our understanding of this region is incomplete. Although it is clear from heterotrimeric structures that G$\beta\gamma$ binding stabilizes the amino-terminal α-helix structure, this may change upon Gα activation. The amino-termini of Gα subunit

* To whom correspondence should be addressed. E-mail: heidi.hamm@vanderbilt.edu, hubbellw@jsei.ucla.edu.

⊥ These authors contributed equally to the presented work.

§ Northwestern University.

|| Vanderbilt University Medical Center.

‡ University of California at Los Angeles.

[1] Abbreviations: G_t, the G protein of rod outer segment, transducin; G_i, a family of G proteins coupled to inhibition of adenylyl cyclase; Gα, the α subunits of various G proteins; G$\beta\gamma$, the $\beta\gamma$ subunit of G proteins; GTPγS, guanosine 5′-*O*-(3-thiotriphosphate); ROS, rod outer segment; SDS, sodium dodecyl sulfate; BSA, bovine serum albumin; HEPES, *N*-(2-hydroxyethyl)piperazine-*N*′-(2-ethanesulfonic acid); EDTA, (ethylenedinitrilo)tetraacetic acid; PMSF, phenylmethylsulfonyl fluoride; DTT, dithiothreitol; MOPS, 3-[*N*-morpholino]propanesulfonic acid; MES, 2-[*N*-morpholino]ethanesulfonic acid; LY, 4-amino-*N*-[3-(vinylsulfonyl)-phenyl]naphthalamide-3,6-disulfonate; RGS, regulator of G protein signaling; SDSL, site-directed spin labeling; EPR, electron paramagnetic resonance; BD: bodipy FL *N*-(2-aminoethyl)maleimide; MB, monochlorobimane; QBB, monobromotrimethylammoniobimane bromide.

10.1021/bi0255726 CCC: $22.00
Published on Web 07/13/2002

families are diverse, varying in their amino acid composition and length. In addition, all Gα subunits are modified at or near their amino-termini by covalent attachment of fatty acids, myristate and/or palmitate. Recently, it has been shown that the amino-terminus plays a part in regulating the activity of $G\alpha_z$ subunits; once Ser 16 of $G\alpha_z$ has been phosphorylated by a p21-activated protein kinase, PAK-1, this $G\alpha_z$ subunit is no longer inactivated by GAP proteins and/or $G\beta\gamma$ subunits, which normally attenuate signaling from Gα subunits (*20*). Together these observations suggest that multiple features within the amino-termini are important in regulation of G-protein function.

In the present study, the solution structure and conformational changes in the amino-terminus of Gα upon activation and upon interaction with $G\beta\gamma$ were investigated. Attention was focused on mutational analysis of the outer solvent-exposed surface of the amino-terminal helix, while leaving intact the inner surface that directly interacts with $G\beta\gamma$. Conformational changes at the amino-terminus were examined by monitoring the fluorescence changes exhibited by an environmentally sensitive fluorescent probe linked to any one of a set of engineered Cys residues within the amino-terminus of $G\alpha_{i1}$. In addition, the EPR properties of nitroxide spin labels attached to the same cysteine residues were used to investigate the conformational changes occurring in this region. These studies allowed a direct examination of amino-terminal conformational changes as they occur in solution, and the results provide insight into dynamic processes which cannot be gleaned from current crystal structures. The fluorescence results lead us to conclude that there is an activation-dependent conformational change occurring in Gα, which results in an increased hydrophobic environment of the amino-terminus after activation. EPR results demonstrate in the GDP bound state the amino-terminus is disordered and becomes α-helical only upon interaction with $G\beta\gamma$, while activation with the non-hydrolyzable activator GTPγS causes the $\alpha\beta\gamma$ complex to dissociate, and the amino-terminus again assumes a random coil conformation.

EXPERIMENTAL SECTION

Materials. Guanosine 5′-*O*-(3-thiotriphosphate) (GTPγS), guanosine 5′-triphosphate (GTP), and guanosine 5′-diphosphate (GDP) were purchased from Boehringer Mannheim (Indianapolis, IN). All restriction and DNA modification enzymes were either from Boehringer Mannheim Biochemicals (Indianapolis, IN) or New England Biolabs (Beverly, MA). Lucifer yellow vinyl sulfone (LY) was purchased from Sigma (St. Louis, MO). The MB (monochlorobimane), QBB (monobromotrimethylammoniobimane bromide), and BD (Bodipy FL *N*-(2-aminoethyl)maleimide) probes were purchased from Molecular Probes (Eugene, OR). The sulfhydryl spin label reagent R1 (*S*-(1-oxy-2,2,5,5-tetramethylpyrroline-3-methyl)methanethiosulfonate) was a generous gift of Prof. Kalman Hideg (University of Pecs, Hungary). All other reagents and chemicals were of the highest purity available.

Preparation of ROS Membranes and $G\beta_1\gamma_1$. Urea washed rod outer segment (ROS) membranes and native $G\beta\gamma$ protein were prepared as previously described (*7*). ROS membranes were aliquoted and stored in a buffer containing 10 mM MOPS, 200 mM NaCl, 2 mM $MgCl_2$, 1 mM DTT, and 100 μM PMSF (phenylmethylsulfonyl fluoride) at −70 °C. Purified $G\beta\gamma$ subunit was stored at −20 °C in a buffer containing 10 mM Tris, pH 7.5, 100 mM NaCl, 5 mM 2-mercaptoethanol, and 40% glycerol.

Construction, Expression, and Purification of Mutant Gα Proteins. An expression vector, which contains $G\alpha_{i1}$ cDNA, was generously provided by Dr. Maureen Linder, Washington University, St. Louis, MO. In this vector, a hexahistadine tag is introduced between amino acid residues M119 and T120 of the $G\alpha_{i1}$ coding region. To be able to specifically label the Gα subunit at the desired cysteine substituted residues, a parent $G\alpha_{i1}$ was generated by removal of reactive cysteines and used as a basis for further mutagenesis. Six out of 10 native cysteines of $G\alpha_{i1}$ were removed using a stepwise mutagenesis approach. To replace Cys^3 with Ser, the forward primer 5′-GGTTTAACCATGGGCTCCACACTGAGCGCTGAGGAC-3′ (underlined nucleotides represent cysteine to serine mutation) and complementary reverse primer were used in the QuickChange (Stratagene, La Jolla, CA) site-directed mutagenesis procedure. Subsequently, native Cys^{66} was replaced by alanine using the forward primer (5′-GCTGGCTACTCAGAGGAAGAGGCTAAGCAGTACAAAGCAGTG-3′) and its complementary reverse primer. Similarly, forward primers for introducing additional mutations C214S, C305S, C325A, and C351I were as follows: 5′-CGGAAGAAGTGGATTCACAGCTTTGAAGGCGTGACTGCC-3′; 5′-GGCGGCTGCGTATATC−CAGAGCCAGTTTGAAGACCTC-3′; 5′-CACCCACTTCACTGCCGCCACGGATACGAAGAAT-GTG-3′; 5′-GAATAACCTAAAAGACATTGGTCTCTTCTAAGCTCTG-CAGTGG-3′. Reverse primers were complementary to the corresponding forward primers. The resulting hexa-mutant $G\alpha_{i1}$−C3S−C66A−C214S−C305S−C325A−C351I (Hexa I) was used as a background for introducing additional cysteine mutations. The presence of mutations was confirmed by DNA sequencing and mutant DNA was then transformed to BL21-(DE3)GOLD cells (Stratagene, La Jolla, CA) for protein expression.

Expression and purification was conducted as described previously (*19*). Briefly, *Escherichia coli* cells were grown to OD_{600} of 0.3 units and then induced with 30 μM IPTG at room temperature for 12−16 h. The recombinant proteins were purified from the soluble fraction by Ni-NTA affinity chromatography (Qiagen, Valencia, CA) according to manufacturer's suggestions with minor modifications. Post-induction cells from a 1 L culture were resuspended in a buffer A (50 mM NaH_2PO_4, pH 8, 300 mM NaCl) containing 5 mM imidazole and protease inhibitors leupeptin, pepstatin, and aprotinin (1 μg/mL), then disrupted by sonication. The cytosolic fraction was incubated with 5 mL of a 50% slurry of Ni-NTA agarose resin for 60 min at 4 °C and loaded onto a column. The unbound proteins were removed by washing first with 20 mL, then 10 mL of buffer A containing 5 mM imidazole and 10 mM imidazole, respectively. Gα mutant proteins were eluted with 5−10 mL of buffer A containing 40 mM imidazole. Eluted proteins were buffer exchanged against buffer B containing 50 mM Tris, pH 8, 50 mM NaCl, 1 mM $MgCl_2$, 20% glycerol, 20 μM GDP, 10 mM 2-mercaptoethanol, and 100 μM PMSF, then loaded onto 8-mL anion exchange column (Waters, Milford, MA) or a 1-mL MonoQ column (Pharmacia Amersham, Piscataway, NJ). A linear 30-mL gradient from buffer B to buffer B containing 200 mM NaCl was applied, and the G protein α subunit

Table 1: Activation-Dependent Fluorescence Changes for LY-Labeled $G\alpha_i$-Hexa I Proteins (% Increase over Basal)[a]

labeled residue	LY fluorescence $G\alpha$-LY + AlF_4^-	LY fluorescence $G\alpha$-LY + $G\beta\gamma$	control: LY fluorescence $G\alpha\beta\gamma$-LY + AlF_4^-	control: intrinsic Trp fluorescence of $G\alpha$-LY + AlF_4^-
3	3.0	19.0	0.2	40
10	14.9	6.5	12.4	41
13	13.5	18.2	14.1	39
14	7.8	5.9	6.7	45
15	3.2	−2.5	1.9	43
16	4.9	10.9	4.0	45
17	12.3	11.5	10.4	42
21	20.8	13.2	20.0	49
29	3.1	0.1	3.9	44

[a] LY fluorescence of the labeled proteins was measured using excitation wavelength of 430 nm while monitoring the emission at 520 nm. Percent increase in fluorescence is relative to the LY fluorescence of GαGDP bound subunit. Data are the average of three independent experiments.

Table 2: Activation-Dependent Fluorescence Changes for Labeled (F)-$G\alpha_i$-Hexa I Proteins (% Increase over Basal)[a]

labeled residue	fluorophore (F)[b]	excitation/ emission	fluorescence $G\alpha$-(F) + AlF_4^-	control: intrinsic Trp fluorescence of $G\alpha$-LY + AlF_4^-
10	MB	378/479	2.38	42
13	MB	378/479	−2.68	48
17	MB	378/479	−0.18	44
21	MB	378/479	−0.68	45
3	QBB	380/475	12.30	48
13	QBB	380/475	4.65	44
17	QBB	380/475	4.32	45
21	QBB	380/475	−16.54	45
10	BD	502/510	66.30	46
13	BD	502/510	32.48	44
17	BD	502/510	23.90	41
21	BD	502/510	5.45	44

[a] Fluorescence of the labeled proteins was monitored at specified excitation and emission wavelengths. Percent increase in fluorescence is relative to labeled (F)-GαGDP bound subunit after subtraction of free probe measured under the same conditions. Data are the average of two to four independent experiments. [b] See Figure 2D.

eluted at approximately 150 mM NaCl. After anion exchange purification, Gα mutants were at least 85−90% pure as estimated by Coomassie blue staining of SDS−polyacrylamide gels. Protein concentration was determined by the Coomassie blue method (*8*) using bovine serum albumin as standard (Pierce, Rockford, IL).

Fluorescent Labeling of Gα Mutant Proteins and Spectrofluorometric Assays. Labeling of Gα proteins with LY was performed as described earlier (*9*). Briefly, a LY stock solution (10 mM) in methanol was added in a 5:1 molar ratio to Gα proteins at a concentration of approximately 1 mg/mL in 50 mM Tris-HCl, pH 8.0, 50 mM NaCl, 1 mM $MgCl_2$, and 50 μM GDP and incubated on ice for 30 min. The labeling reactions were quenched by addition of β-mercaptoethanol to a final concentration of 5 mM. The excess fluorescent compound was removed by overnight dialysis. The stoichiometry of the LY labeling was calculated as a molar ratio of the concentration of LY to the concentration of the labeled protein. The concentration of LY was determined by measuring the absorbance of labeled protein at 430 nm using an LY extinction coefficient of 12 400. The protein concentration of labeled samples was determined by the Coomassie blue binding method (*8*). Labeling stoichiometry of all the samples was between 0.4 and 0.6 mol/mol. Labeling with MB, QBB, and BD was performed as described above, with the following modifications: MB and BD were dissolved in DMSO to prepare stock labeling solution, while QBB was dissolved in buffer. After dialysis, excess free fluorescent probe was removed by HPLC chromatography on a Tosoh Haas TSK super SW2000 gel filtration column. Extinction coefficients for MB, QBB, and BD are 6000, 5580, and 79 000 cm^{-1} M^{-1}, respectively. Stoichiometry of labeling was >0.5 mol/mol for MB, QBB, and BD labeled mutants.

To monitor the ability of Gα mutants and labeled Gα mutants to undergo activation, intrinsic tryptophan (Trp^{207}) fluorescence of the proteins (100 nM) was monitored in buffer B by excitation at 280 nm and emission at 340 nm before and after the addition of AlF_4^- (10 mM NaF + 50 μM $AlCl_3$) using an AMINCO Bowman series 2 Luminescence spectrometer. LY fluorescence of the labeled proteins was measured in buffer B using excitation at 430 nm and emission at 520 nm before and after the addition of AlF_4^- or $G\beta\gamma$ subunit. MB, QBB, and BD were monitored in the same manner at excitation and emission wavelengths specified in Table 2.

Native PAGE. To determine binding of LY labeled $G\alpha_i$ Hexa I subunits to $G\beta\gamma$, a 2:1 molar excess of $G\beta\gamma$ to $G\alpha_i$ Hexa I mutant protein were incubated at 4 °C and then run on a 4−12% tris-glycine gel in the absence of β-mercaptoethanol and SDS. Illumination by UV light, followed by Coomassie staining, was used to visualize complexes containing the LY-labeled proteins.

GTPγS Binding Assay. To determine the rate of rhodopsin-dependent GTPγS binding, sample proteins (4 μM) were preincubated with $G\beta\gamma$ (4 μM) and dark rhodopsin (400 nM) in 50 μL of buffer containing 100 mM HEPES, pH 8.0, 1 mM EDTA, 10 mM $MgSO_4$ and 10 mM DTT (dithiothreitol)

for 30 min on ice as described earlier (*19*). After preincubation, the samples were exposed to light and the reaction was started by the addition 150 μL of [^{35}S]GTPγS (final concentration 5 μM; ~5000 cpm/pmol). Aliquots (20 μL) were withdrawn at the indicated times, passed through the Millipore Multiscreen-HA 96-well filtration plate, and washed 5 times with 150 μL of ice cold wash buffer containing 20 mM Tris-HCl, pH 8.0, 100 mM NaCl, and 25 mM $MgCl_2$. Filters were dried, punched by Millipore Multiscreen Puncher, and counted.

GTPase Activity Assay. Intrinsic GTPase activity of Gα proteins (200 nM) was measured in a buffer containing 50 mM HEPES, pH 8.0, 5 mM EDTA, 0.05% Tween-20, 1 μM [γ^{32}P]GTP (~8000 cpm/pmol), 1 μM AMP−PNP, and 1 mM DTT. The reaction was initiated by the addition of 15 mM $MgCl_2$ and 100 μM GTPγS. RGS4 stimulated GTPase activity was measured with the same procedure; in this experiment, 200 nM RGS4 was added to the initial mixture of $MgCl_2$ and GTPγS. Fifty microliter aliquots were withdrawn at the indicated times and quenched by the addition of 100 μL of 7% perchloric acid. Nucleotides were removed by the addition of 500 μL of a 10% solution of activated charcoal, and the free $^{32}P_i$ was measured by scintillation counting.

Spin Labeling and EPR Measurements. Prior to the labeling reaction, Gα subunits were diluted with the labeling buffer containing 10 mM MES (pH 6.8), 100 mM NaCl, 5 mM $MgCl_2$, 100 μM GDP, and 10% glycerol (w/v) to a final volume of 500 μL. DTT was then added to a final concentration of 10 mM, and the sample was incubated at room temperature for 10 min. Excess DTT was removed on a Hi-Trap column (Amersham Pharmacia Biotech, Piscataway, NJ), and the sample was concentrated to a final volume of 500 μL using a Centricon-10 filtration unit (Millipore, Bedford, MA). For the spin-labeling reaction, the sulfhydryl reagent *S*-(1-oxy-2,2,5,5-tetramethylpyrroline-3-methyl)-methanethiosulfonate was added in a 1:1 molar ratio of spin label/protein, and the samples were incubated at room temperature for 10 min. Any excess spin label was removed and the buffer exchanged on a Hi-trap column eluting with 10 mM MES (pH 6.8), 100 mM NaCl, 5 mM $MgCl_2$, 100 μM GDP, and 10% glycerol.

For EPR spectroscopy, the Gα samples (typically 300 μL at a concentration of 2−8 μM labeled protein) were loaded into a quartz flat cell contained in a TM rectangular cavity fitted with an optical window. Spectra were recorded at room temperature at X-band microwave frequency using a Varian E-109 spectrometer with 10 mW incident power under field-frequency lock conditions. Field modulation amplitudes were optimized for each sample to provide maximum signal without distortion of the line shape. After recording the spectrum, each Gα sample was recovered and G$\beta\gamma$ added in equimolar amounts, after which the sample was concentrated to the original volume and the spectrum recorded. The sample was again recovered and dark urea-washed ROS membranes added in excess, and the spectrum recorded both in the dark and following photobleaching for 1 min with a 100W halogen source filtered with an infrared block and a long-pass filter (λ > 500 nm). Finally, GTPγS was added to a final concentration of 0.5 mM, the mixture incubated for 20 min at 4 °C, and the spectrum recorded at room temperature.

Experimental EPR spectra were fit in a least-squares sense to the microscopic order macroscopic disorder (MOMD) model of Freed and co-workers using a single term in the ordering potential (c_o2), corresponding to a single order parameter to describe the motion (*15*). For the R1 nitroxide side chain at solvent-exposed helical sites, the principle values of the **g** and **A** tensors are $g_{xx} = 2.0076$, $g_{yy} = 2.0050$, $g_{zz} = 2.0023$, $A_{xx} = 6.2$ G, $A_{yy} = 5.9$ G, $A_{zz} = 37$ G, and the tilt angle between the diffusion tensor and the nitroxide molecular frame (β_D) is 37° (*16*). The fitting procedure gives values of the order parameter and the diffusion tensor of the nitroxide, D_{xx}, D_{yy}, D_{zz}. The effective correlation time is defined as $\tau_{eff} = 1/6(D_{xx}D_{yy}D_{zz})^{1/3}$.

RESULTS

Determination of Reactive Cysteines in Gα_{i1}. To investigate the role of the amino-terminus of G protein α subunit in activation-dependent conformational changes and to examine its dynamic molecular interaction with G$\beta\gamma$ subunit and rhodopsin, we performed a site-directed cysteine mutagenesis study of this region. Gα_{i1} is a close relative of retinal rod cell transducin Gα_t and functionally couples almost as well as G_t to rhodopsin (data not shown). Due to higher yields of Gα_{i1} than Gα_t expression in *E. coli*, we decided to make our set of amino-terminal region mutants in the context of Gα_i. Native Gα_{i1} protein contains 10 cysteine residues: C3, C66, C139, C214, C224, C254, C286, C305, C325, and C351. To use a cysteine-directed labeling approach, a mutant Gα_{i1} without reactive cysteines was generated. A similar G$\alpha_{i/t}$ chimera has only three cysteine residues available for labeling (*9*); therefore, we initially made the triple mutant of Gα_{i1}, Gα_{i1}−C3S−C214S−C351I.). However, unlike earlier studies on a similar G$\alpha_{i/t}$ chimera (*9*), three additional cysteines (C66, C305, and C325) had to be removed from the Gα_{i1} protein before it was nonreactive with cysteine-directed labels. Most surface-exposed cysteines can be conservatively replaced by serine, but metarhodopsin II stabilization assays indicated that substitutions C351I, C66A, and C325A better preserved coupling to rhodopsin than the serine substituted counterparts (data not shown), likely due to the slightly more hydrophobic environment of these residues in the native protein. The resulting mutant Gα_{i1}−C3S−C66A−C214S−C305S−C325A−C351I (Hexa-I) had functional properties very similar to that of native Gα_i (Figure 1A−C) and provided a background against which later mutations were made.

Functional Assays. To determine whether the mutant protein folded properly, had GDP bound, and could undergo a GTP-dependent conformational change, the intrinsic fluorescence change of Trp^{207} after addition of AlF_4^- was measured. The Hexa I protein underwent a conformational change upon binding to AlF_4^-, resulting in about 45% relative increase in fluorescence for both Hexa I and wild-type recombinant Gα_{i1} proteins (Figure 1A). To determine the ability of the Hexa I mutant to interact with G$\beta\gamma$ and activated rhodopsin, the rate of rhodopsin-catalyzed exchange of GDP for [^{35}S]GTPγS was measured (Figure 1B). The addition of equimolar concentrations of G$\beta\gamma_t$ (1 μM) and 100 nM rhodopsin to Gα_t, Gα_{i1}, or Hexa I caused stimulation of GTPγS binding to all proteins with the apparent rate constants of 0.60, 0.31, and 0.35 min^{-1}, respectively. Despite Gα_i's slightly lower rate of rhodopsin catalyzed exchange

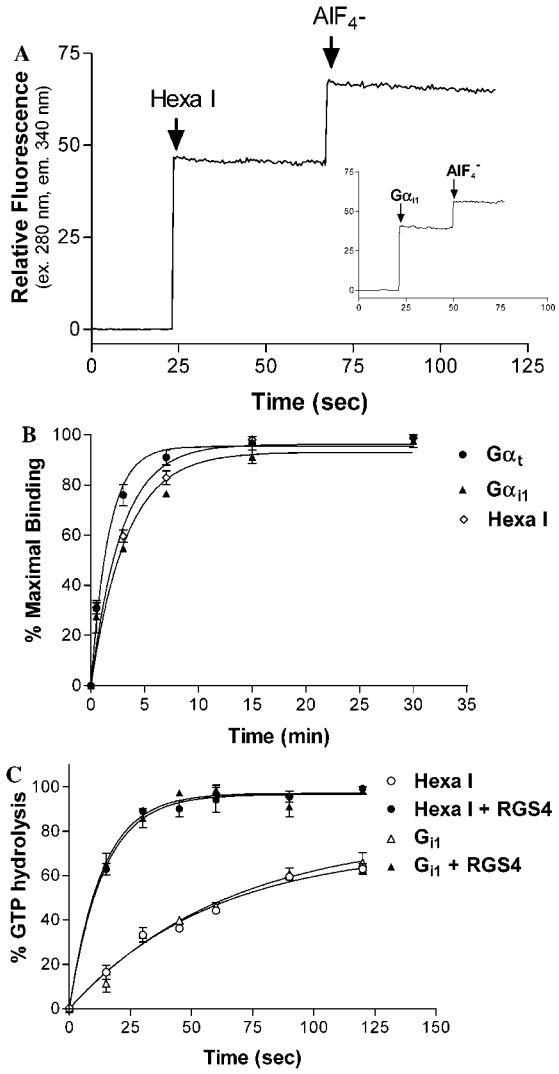

FIGURE 1: (A) Intrinsic Trp fluorescence changes induced by AlF_4^- activation of Hexa I mutant of $G\alpha_{i1}$-GDP. Fluorescence measurements were carried out as described under Experimental Procedures. Gα protein (100 nM) was activated in 50 mM Tris-HCl, pH 8.0, 50 mM NaCl, 2 mM $MgCl_2$, 50 μM GDP, and 0.1 mM phenylmethylsulfonyl fluoride by AlF_4^- (10 mM NaF + 50 μM $AlCl_3$). Fluorescence was measured by excitation at 280 nm and emission at 340 nm before and after the addition of AlF_4^- using an AMINCO Bowman Series 2 Luminescence spectrometer. (B) Time course of GTPγS binding to $G\alpha_t$ (filled circles), $G\alpha_{i1}$ (triangles), and Hexa I (open circles). Gα proteins (1 μM) in the presence of 100 nM rhodopsin and 1 μM $G\beta\gamma_t$ were incubated at room temperature in buffer containing 100 mM HEPES, pH 8.0, 1 mM EDTA, 10 mM $MgSO_4$, 1 mM DTT, and 5 μM [^{35}S]GTPγS. Duplicate aliquots were withdrawn at the indicated times, filtered, and counted. Binding of GTPγS is expressed as percent of maximal and fit using nonlinear least squares criteria to the equation $B = B_{max}(1 - e^{-kt})$. Data shown represents mean of two independent experiments. (C) Intrinsic and RGS4 stimulated GTPase activity of wild-type $G\alpha_{i1}$ (triangles) and Hexa I mutant (circles). GTPase activity of Gα proteins (200 nM) (circles, Hexa I; triangles, $G\alpha_{i1}$) as measured in a buffer containing 50 mM HEPES, pH 8.0, 5 mM EDTA, 0.05% Tween-20, 1 μM [γ^{32}P]GTP (~10^4 cpm/pmol), 1 μM AMP-PNP, and 1 mM DTT. Reaction was started by addition of 15 mM $MgCl_2$ and 100 μM GTPγS with (closed symbols) or without (open symbols) 200 nM RGS4. Aliquots were withdrawn at the indicated times and quenched by the addition of 100 μL of 7% perchloric acid. Nucleotides were removed by activated charcoal, and free $^{32}P_i$ was measured by scintillation counting. GTP hydrolysis is expressed as percent of maximal and fit using nonlinear least squares criteria to the equation $B = B_{max}(1 - e^{-kt})$. Data shown represents mean of two independent experiments.

of GDP for [^{35}S]GTPγS compared to that of $G\alpha_t$, we did not observe any additional decrease due to the presence of multiple mutations in $G\alpha_{i1}$ Hexa I protein. To further demonstrate that the Hexa I mutant was fully functional, we measured its intrinsic and regulator of G-protein signaling 4 (RGS4) protein stimulated GTPase activity. The Hexa I mutant behaved essentially the same as native $G\alpha_{i1}$, both in the absence and in the presence of the RGS4 protein (Figure 1C).

Strategy for Studying the Activation Dependent Conformational Changes of the Amino-Terminus of the Gα Subunit. To address the role of Gα amino-terminus in G-protein activation, a site-directed cysteine mutagenesis study of the amino-terminus of Gα subunit was carried out. Additional cysteine incorporating mutations were introduced at multiple solvent-exposed positions opposite the Gβγ binding interface on the amino-terminal helix (Figure 2A,B). Nine mutants along the surface of the amino-terminal helix in the context of Hexa I were prepared: Hexa I-3C, where a native cysteine was introduced back into the structure, Hexa I−K10C, Hexa I−V13C, Hexa I−E14C, Hexa I−R15C, Hexa I−S16C, Hexa I−K17C, Hexa I−R21C and Hexa I−K29C. Mutant proteins were expressed and purified from *E. coli* (Figure 2C). All mutants appeared to be properly folded and functionally active as judged by the change in intrinsic Trp fluorescence after the addition of AlF_4^- (Figure 2C). Conformational changes associated with G-protein activation were detected through attachment of a thiol reactive environmentally sensitive probe, Lucifer yellow (LY). LY is a sensitive reporter of environmental changes; its fluorescence emission increases when it moves into a more hydrophobic environment. LY, as well as other thiol-reactive fluorescent probes used in this study are shown in Figure 2D. The fluorescently labeled mutants retained the ability to change conformation upon activation with AlF_4^-; the increase in intrinsic Trp^{207} fluorescence of the fluorescently modified proteins after the addition of AlF_4^- was again about 40% (Tables 1 and 2).

Binding of Hexa I Mutants to Gβγ. To confirm the binding of LY-Hexa I mutants to Gβγ, the labeled subunits were incubated with Gβγ and complexes identified with native PAGE electrophoresis. The resulting UV and Coomassie stained gels demonstrated that the labeled subunits bound Gβγ subunits quantitatively; no free Gα was evident after incubation and electrophoresis of excess Gβγ with any of the LY-Hexa I Gα proteins (Figure 2E, upper panel). In a similar control experiment, native $G\alpha_i$ (Figure 2E, far right, lane 1) was incubated with excess Gβγ (lane 2); the resulting reconstituted heterotrimer (along with free Gβγ) is in lanes 3 and 4. Although Gβγ does not show altered mobility upon binding Gα under these conditions, no free, unbound Gα subunits are seen in any lanes containing Gβγ. A 2-fold molar excess of Gβγ to Gα subunits resulted in loss of free Gα in the native gel due to quantitative Gα binding to Gβγ (Figure 2E, upper right) and LY-labeled Hexa I proteins (Figure 2E, upper left panel). UV illumination of the gels prior to staining confirm the presence and electrophoretic position of the LY-labeled Gα subunits (Figure 2E, lower panel). In a similar experiment, gel filtration chromatography of the reconstituted heterotrimer consisting of Hexa I C21LY-$G\beta_1\gamma_1$ eluted at the same retention time as native G_t heterotrimer obtained from native bovine rod outer segments (data

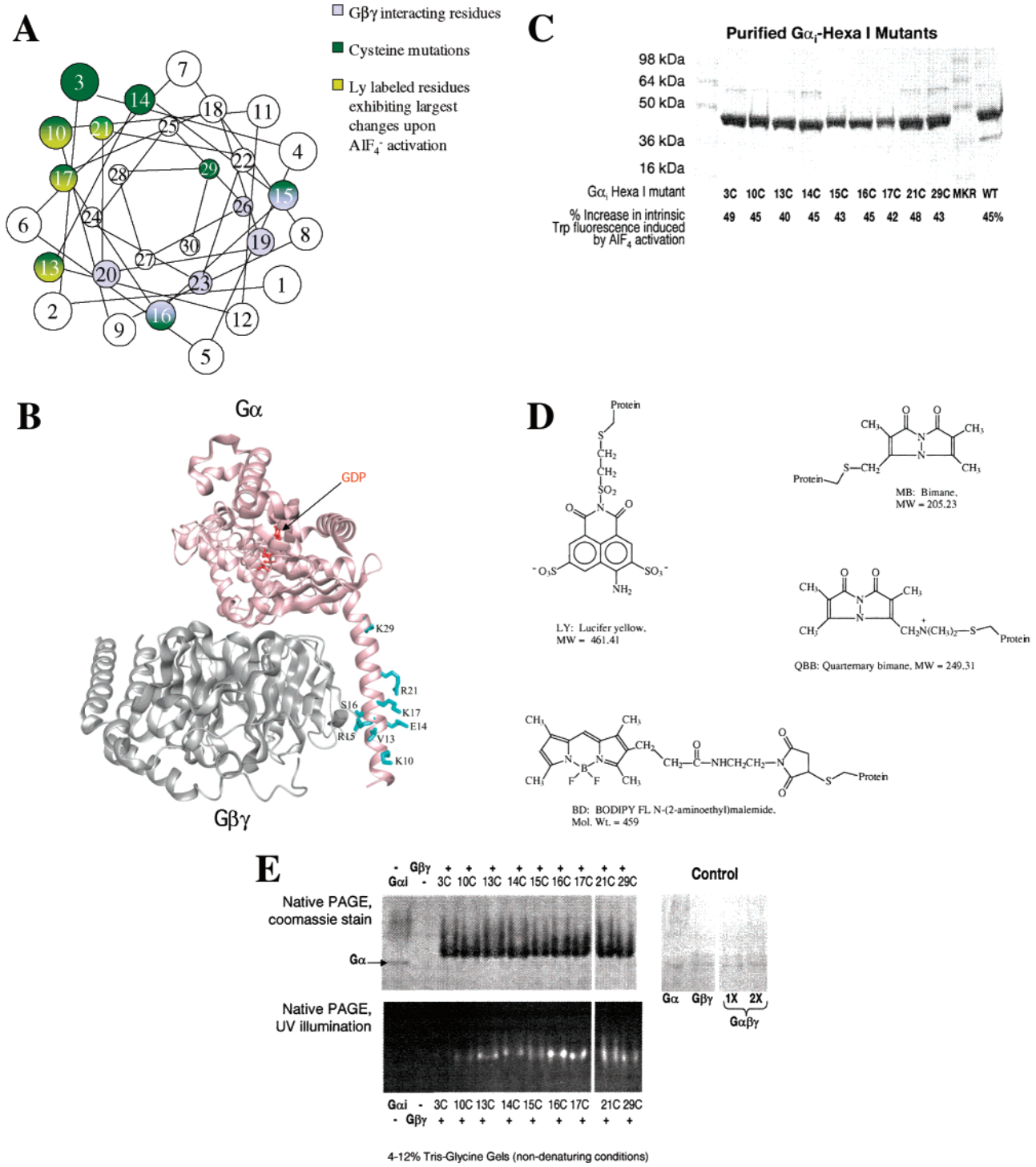

FIGURE 2: (A) α-Helical wheel model for the amino-terminal 30-amino acid region of $G\alpha_{i1}$. $G\beta\gamma$-interacting residues are shown in blue, Cys mutations are shown in green, and residues with the greatest AlF_4^--induced increase in fluorescence are shown in yellow. (B) Visualization of $G\alpha_i$ complexed with $G\beta\gamma$ using DINO, PDB file 1GP2. (C) (Upper panel) Expression of $G\alpha_i$ and purification as described in methods resulted in ~90% pure recombinant $G\alpha_i$ protein as estimated from Coomassie stained SDS−PAGE gel. (Below) Describes typical intrinsic Trp^{207} fluorescence increase after AlF_4^- activation for each of the purified $G\alpha_i$ Hexa I subunits. (D) Fluorescent probes used in this study. (E) Native PAGE gels demonstrate binding of LY-labeled $G\alpha_i$ Hexa I mutants to $G\beta\gamma$ subunits. (Upper panel): Subunits were incubated in a 2 molar excess of $G\beta\gamma$ to Gα at 4 °C for 10 min, followed by electrophoresis at 100 V for 2 h in the absence of SDS and reducing agents. (Lower panel): UV illumination prior to Coomassie staining confirms labeling and electrophoretic mobility of LY-$G\alpha_i$ Hexa I proteins.

not shown). These somewhat anomalous migrations of heterotrimer in native gel and gel filtration chromatography agree with sedimentation analysis, which reveals similar sedimentation coefficients for $G\alpha_t$-GDP, $G\beta\gamma$, and the reconstituted heterotrimer, and an anomalously long RT for the heterotrimer upon gel filtration chromatography (*21*).

Effect of Gα Activation on the Fluorescence of Site-Specific Fluorescent Labels. To determine whether there was an activation-dependent conformational change in or around the amino-terminus of Gα, we first measured the LY fluorescence change of labeled amino-terminal $G\alpha_{i1}$ mutants upon addition of AlF_4^- (Table 1). We found changes in

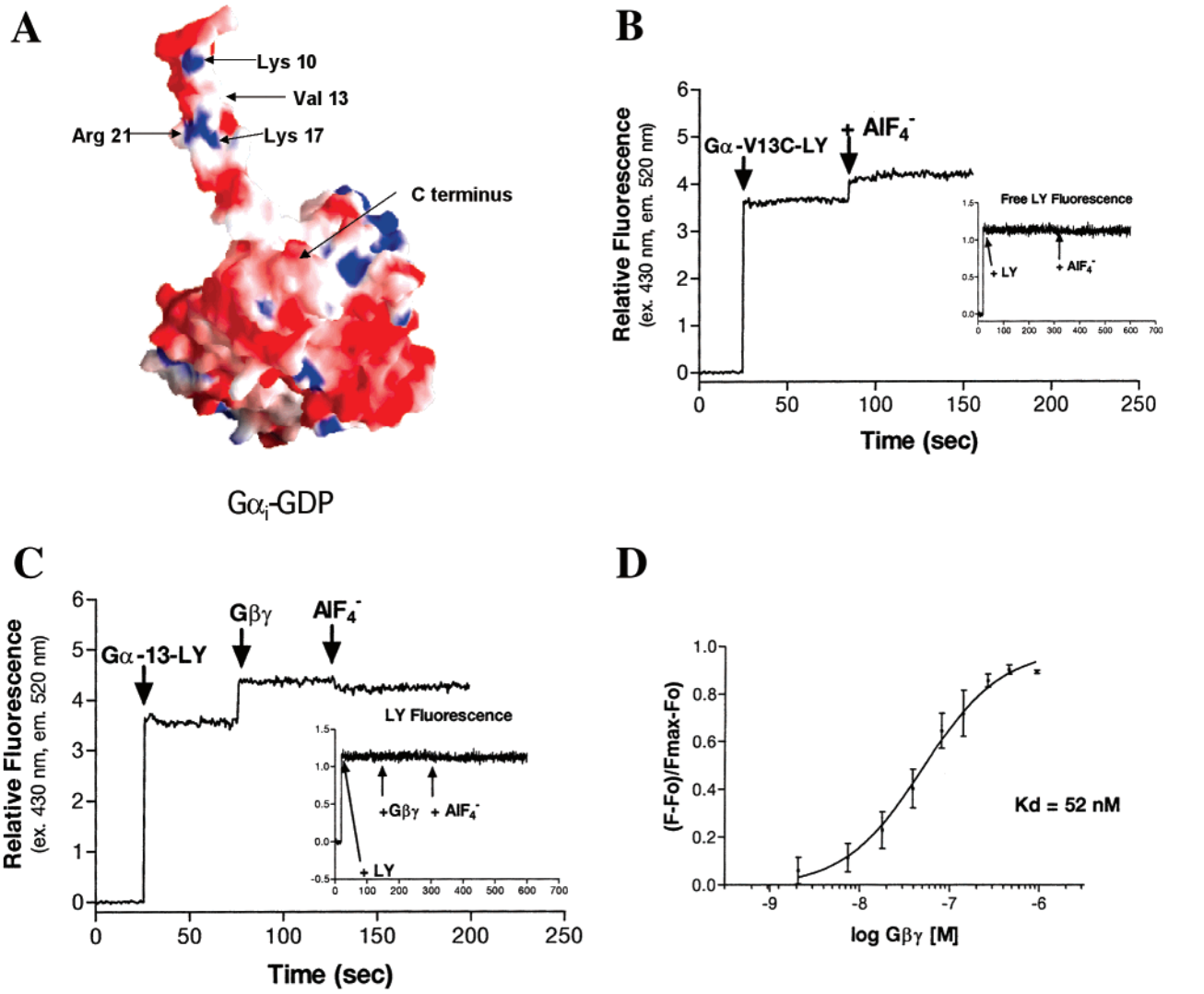

FIGURE 3: AlF_4^-- and G$\beta\gamma$-dependent fluorescent changes of Hexa I-V13C mutant specifically labeled at the position 13 with Lucifer yellow. (A) Electrostatic (red acidic, blue basic) surface potential diagram of inactive $G\alpha_{i1}$ in the context of the heterotrimer using GRASP, PDB file 1GP2. (B) The LY fluorescence (excitation 430 nm; emission 520 nm) of fluorescently labeled Hexa I-V13C-LY subunit (100 nM) alone and upon activation with AlF_4. Inset: fluorescence of LY label alone and after addition of AlF_4^- to the cuvette. (C) LY fluorescence of Hexa I-V13C-LY (excitation 430 nm; emission 520 nm) subunit upon binding to G$\beta\gamma$ subunit (200 nM) and after activation of the reconstituted heterotrimer with AlF_4^-. Inset: fluorescence of LY label alone, after addition of G$\beta\gamma$, and after a final addition of AlF_4^- to the cuvette. (D) Affinity of labeled Hexa I subunits for G$\beta\gamma$. Relative fluorescence change of Gα-V13C-LY represented as a function of G$\beta\gamma$ concentration. Gα-V13C-LY (16.6 nM) was incubated with G$\beta\gamma$ concentrations ranging from 1 nM to 1 μM in buffer B. LY fluorescence (F) of the labeled protein was monitored (ex. 430 nm, em 520 nm) both before and after indicated additions of G$\beta\gamma$, and results plotted as percent of maximum increase.

fluorescence of LY-labeled amino-terminal residues ranging from 3 to 20% for these solvent-exposed residues upon activation. The largest AlF_4^--dependent fluorescent increases in LY-labeled proteins were found at positions 10, 13, 17, and 21 (Figure 2A). To rule out aggregation as an artifactual cause of increased fluorescence upon activation, gel filtration chromatography of $G\alpha_i$-Hexa I 21CLY-GDP in the presence and absence of AlF_4^- was conducted. GDP bound $G\alpha_i$ Hexa I 21C-LY and GDP-AlF4 bound $G\alpha_i$ Hexa I 21C-LY eluted at 10.35 and 10.48 min, respectively. This correlates to a molecular mass equal to that of the Gα subunit, approximately 39 kDa, thus demonstrating the monomeric nature of both the GDP bound and GDP-AlF_4^- -activated subunits.

Since the measured increases in fluorescence indicate an increased hydrophobic environment for the LY-labeled residues, and since addition of AlF_4^- prevents rather than causes oligomerization of Gα subunits (*21*), there must be an intramolecular site on $G\alpha_i$ that the amino-terminal region binds upon activation. The amino-terminus may bind in an extended conformation; residues examined so far may not include those that most closely approach the body of the Gα protein. To localize these four residues on the structure, a GRASP[2] view of $G\alpha_i$-GDP in its heterotrimeric conformation was examined (Figure 3A). The surface potential shows that these residues form a positive patch on the helical amino-terminal region.

A representative example of the experimental fluorescence data for one of the labeled amino-terminal mutants (Hexa

[2] Modeling programs: electrostatic surface: GRASP, Nicholls, A., Sharp, K., Honig, B. (1991) *Proteins: Struct., Funct., Genet. 11* (4), 281; 3D structures, DINO: Philippsen, A. (2001) Division of Structural Biology, Biozentrum, University of Basel, Switzerland; Visualizing Structural Biology, http://www.dino3d.org.

I-V13C-LY) is presented in Figures 3B−D. Upon addition of AlF_4^- to the LY-labeled Hexa I-V13C protein, the relative fluorescence increased about 14%, indicating a more hydrophobic environment for this labeled residue upon activation. Significant changes in fluorescence were also observed for Bodipy labeled mutants (Table 2), while smaller fluorescent probes registered fluorescent changes to a lesser degree upon activation.

Since the heterotrimer structure shows the amino-terminus of Gα is a part of the interaction interface with the G$\beta\gamma$ subunit (*1*, *2*) (Figure 2B), we measured the fluorescence change of the labeled mutants upon interaction with the G$\beta\gamma$ subunit (Table 1). Figure 3C is an example of the fluorescence data obtained for Hexa I-V13C-LY upon G$\beta\gamma$ interaction. The amino-terminal Val 13, while not a direct part of G$\beta\gamma$'s interacting surface, is located on the inner surface of the helix, close to G$\beta\gamma$ interacting residue Asp 20. Upon addition of the G$\beta\gamma$ subunit to the cuvette, the fluorescence of the LY label attached to C13 increased about 18%. We observed slightly smaller increases in fluorescence for the mutants where the label was placed on residues more distant from the G$\beta\gamma$'s binding interface (Table 1).

The largest increase in LY fluorescence upon G$\beta\gamma$ addition came from a labeled residue at the extreme amino-terminus, Hexa I-3C (Table 1). This result is in contrast to residue 14, which lies directly opposite the G$\beta\gamma$ binding interface on the helix. This LY-labeled solvent-exposed residue registered only a small change in its environment upon binding to G$\beta\gamma$ and upon activation by AlF_4^-. In both the active and inactive states, this residue remained oriented primarily toward the bulk of the solution, albeit to a lesser extent in the GDP-AlF_4^- and G$\beta\gamma$ bound states than in the GDP bound state (Table 1).

After addition of AlF_4^- to the LY-G$\alpha\beta\gamma$ complex, the LY fluorescence of the mutants returned to approximately the same value exhibited after AlF_4^- activation of the free α subunit (Figure 3B,C, and Table 1). This AlF_4^--dependent dissociation of Gα from the heterotrimer is another measure of the functional integrity of the labeled Gα subunits. The fluorescence changes exhibited by the labeled proteins are in contrast to control experiments with AlF_4^- added to LY alone (Figure 3B, inset), AlF_4^- added to a G$\beta\gamma$ and LY mixture (Figure 3C, inset), and AlF_4^- added to G$\beta\gamma$ alone, as well as AlF_4^- added to a mixture of Gα and nonreactive LY where no fluorescent change was detected (results not shown).

To measure the affinity of the binding of LY-labeled $G\alpha_i$ Hexa I subunits to G$\beta\gamma$, the fluorescence of $G\alpha_i$ Hexa I-V13C-LY was measured alone and in the presence of increasing amounts of G$\beta\gamma$ (Figure 3D). A dose-dependent increase in LY fluorescence was seen as the Hexa I-V13C-LY subunit bound G$\beta\gamma$ with a K_d value of 52 nM for binding, similar to a value of 24 nM found by using Western blots to detect binding of the 41 kDa $G\alpha_i$ subunit to G$\beta\gamma$ (*17*). This is somewhat less than the affinity measured by flow cytometry in a lipid environment (2.9 nM), which would be expected to enhance interactions between myristoylated, native $G\alpha_i$, and prenylated G$\beta\gamma$ (*18*).

Spin Labeling and Electron Paramagnetic Resonance Spectroscopy of the Labeled Mutants. To further examine the conformation of the Gα amino-terminal sequence under various conditions, the cysteine mutants in the Hexa I background were modified with a nitroxide methanethiosulfonate reagent to generate the spin-labeled side chain designated R1 (Figure 4A). Figure 4B−E shows the EPR spectra of $G\alpha_i$ derivatives 10R1, 13R1, 14R1, and 21R1 in buffer (green trace) and after the addition of stoichiometric quantities of G$\beta\gamma$ (blue trace).

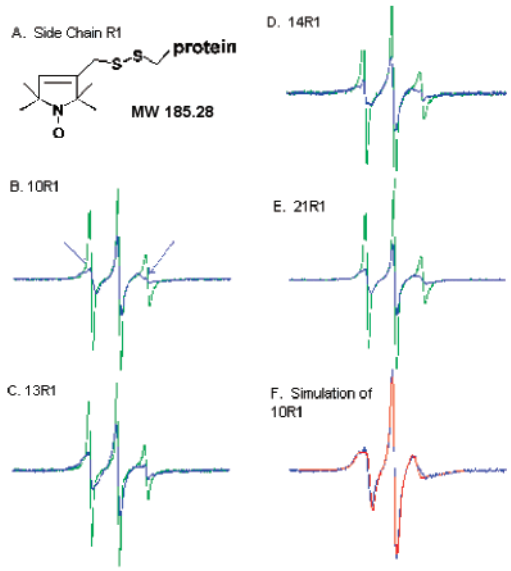

FIGURE 4: EPR spectra of spin labeled mutants of Gα-GDP. (A) Structure of the R1 side chain. (B−E) Spectra of the indicated mutants of Gα, either alone in solution (green trace) or after addition of stoichiometric amounts of G$\beta\gamma$ to form the G$\alpha\beta\gamma$ complex (blue trace). The arrows in the spectra for the G$\alpha\beta\gamma$ complex in panel B indicate the presence of a small amount of unbound Gα subunit; similar components are present in the other mutants. (F) The experimental spectrum of 10R1, after spectral subtraction of the small amount of unbound component (blue trace), and the simulated spectrum for an R1 side chain at a helix surface site with $S = 0.46$ and $\tau_{eff} = 1.6$ ns (red trace). Details of the simulation parameters are in the Experimental Section.

For the Gα-GDP subunit alone in buffer, the EPR spectra are similar for each mutant, and represent rapid, essentially isotropic, motion of the side chain. The correlation times are in range 0.7−0.9 ns, similar to those for R1 residues in the disordered C-terminal domain of rhodopsin (*13*) and unfolded proteins (*14*). Assuming Stokes−Einstein behavior, the correlation time for Gα in 10% glycerol at room temperature (viscosity 1.3 cp) is estimated to be $\tau_c \approx 14$ ns. Thus, the much shorter correlation times observed experimentally for R1 must reflect internal motions within Gα. Upon addition of G$\beta\gamma$, the motion of R1 slows drastically, reflecting the formation of an ordered structure (Figure 4, blue traces). On the basis of the crystal structure of the heterotrimer, the structure is expected to be a regular α-helix. The EPR spectra are consistent with this expectation in two ways. First, the motion of R1 at each site, inferred from the spectral line shapes, is consistent with a location on the solvent-exposed surface of a α-helix. The spectra of R1 on helix surface sites arise from an anisotropic motion dictated by restricted torsional oscillations about the two terminal bonds in the side chain (*16*), and the fits of the spectra for R1 in G$\alpha\beta\gamma$ to this model are good. An example fit is shown in Figure 4F for 10R1. The others can be similarly fit, although in 13R1 and 14R1 there are small additional spectral components due to weak side chain interactions. In the case of 10R1, the simulated spectrum was generated using an

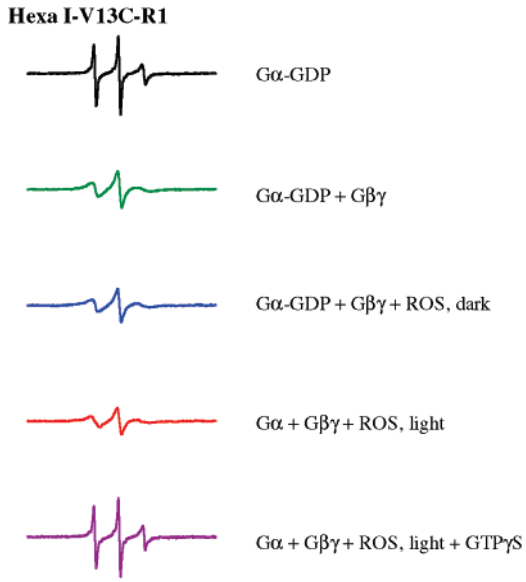

FIGURE 5: EPR spectra of 13R1. EPR spectra for Gα-GDP 13R1 alone (≈10 μM, first panel) and for Gα-GDP 13R1 after the indicated additions. For G$\beta\gamma$, the addition was stoichiometric. For addition of urea-washed ROS, the rhodopsin was in large excess over Gα. GTPγS concentration was 1 mM. Experimental conditions are described in Experimental Section.

order parameter $S = 0.46$ and an effective correlation time $\tau_{eff} = 1.6$ ns. For an R1 residue in a rigid helix, namely, 72R1 in T4 lysozyme, the order parameter is similar ($S = 0.47$), but the correlation time is longer ($\tau_{eff} = 2.2$ ns) (*16*). Thus, if the amino-terminal structure is indeed helical, it is not rigid, but has dynamic modes due to backbone fluctuations that are reflected in the rate of side chain motion.

The sequence-dependence of the data in Figure 4 is also consistent with an amino-terminal helix in the G$\alpha\beta\gamma$ complex. This is so because each of the sites investigated was selected from the crystal structure to lie on the solvent-exposed face of the amino-terminal helix, and the EPR data are consistent with this assignment.

The EPR spectra for R1 in the heterotrimeric complex contain two components, one corresponding to a helix surface site (dominant), and the other to a much more mobile state, similar to that in Gα-GDP alone (arrows, Figure 4B). This latter component is no more than a few percent of the population. For a K_d of 52 nM (see Figure 3D) and the concentrations employed in the EPR experiments, this population is consistent with the amount of Gα-GDP in equilibrium with the heterotrimer.

Figure 5 shows an example (for 13R1) of the EPR spectral changes observed when a spin-labeled Gα subunit is followed through a series of transformations relevant to signal transduction in context of the receptor, rhodopsin. The first two panels show the change just discussed due to complex formation with G$\beta\gamma$. As shown in the third and fourth panel, there is very little change upon addition of urea-washed, dark ROS membrane or upon subsequent photobleaching. However, addition of GTPγS after photobleaching caused a dramatic change from the helix-like structure of the amino-terminus back to a highly dynamic, disordered structure indistinguishable in its EPR spectrum from the Gα-GDP, again demonstrating the GTP-dependent dissociation of Gα and G$\beta\gamma$ heterotrimer. Figure 5 highlights the spectral line shape changes as the amino-terminus moves from a random coil in the Gα-GDP bound form to an ordered α-helix in the $\beta\gamma$ bound form of Hexa I-V13C-R1.

A further EPR experiment performed in a similar manner was carried out on $G\alpha_i$ Hexa I 17C-R1-GDP in which AlF_4^- was substituted for GTPγS. There was no change in the order of the spin label upon activation with AlF_4^-. This is due to the inability of a small spin label to report changes in polarity of its environment in the absence of any direct interaction involving the spin label, in contrast to longer, more extended environmentally sensitive fluorescent probes which are quite sensitive to changes in the overall environment of the probe.

DISCUSSION

As demonstrated by the crystal structure of the heterotrimeric G protein (*1*, *2*), the amino-terminus of Gα subunits forms an α-helix interacting with the G$\beta\gamma$ subunit. However, little is known about the conformation of the amino-terminal region in Gα-GTP bound state, since in reported crystal structures this region is either missing or not significantly resolved. Both $G\alpha_t$-GTPγS and $G\alpha_t$-GDP crystals are missing 23 residues from the amino-terminus. Furthermore, neither the crystal structures of the Gα subunit nor that of the heterotrimeric G proteins show the conformation of the first four amino acid residues of the subunit (*1*, *2*). Thus, the secondary structure and folding of Gα amino-terminus in the absence of the G$\beta\gamma$ subunit are not known. The crystal structure of a recombinant $G\alpha_{i1}$ reveals its amino-terminus folding back in the GDP bound state to form an α-helix organized in a compact microdomain with the carboxyl terminus. This may demonstrate the instability of the amino-terminus in the absence of G$\beta\gamma$, or may simply be an artifact of crystallization. By systematically examining the environment of solvent-exposed residues in the amino-terminal helix, we were able to detect activation-dependent changes occurring in this region, supporting the hypothesis that there is a conformational change in the amino-terminus upon activation.

The EPR results indicate that both GDP and GTPγS bound amino-terminal mutants have a random coil structure. Details from fluorescence studies aimed at examining subtle changes in the environment of labeled residues suggests the amino-terminus is somewhat more solvent exposed in the GDP bound form than in the GTP/GDP-AlF_4^- activated state, and this can be seen in the relatively increased fluorescence of the labeled residues in the GTP/AlF_4^- bound state as compared to the GDP bound state (Table 1). This increase in relative fluorescence of labeled cys-substituted amino-terminal mutants after AlF_4^- activation indicates an increased hydrophobic environment of the probe after activation, which suggests that the conformation of the amino-terminus in the inactive GDP bound and active GDP-AlF_4^- state might differ.

Since there are no other proteins or lipids in this part of the experiment, it is conceivable that in the active Gα conformation, the amino-terminus may have an intramolecular binding site on the Gα molecule. Analysis of the EPR spectra of the mutants suggests that an ordered amino-terminal helix is present only when the Gα subunit is bound to G$\beta\gamma$, and this region is highly mobile in either the Gα-GDP or Gα-GTPγS bound state. This would seem to contradict the fluorescence evidence that LY-labeled residues 10, 13, 17, and 21 move into a more hydrophobic environ-

ment in the activated state. This does not rule out the possibility that the charged fluorescent probe, larger than the nitroxide label, may be stabilizing a weak interaction not seen with the smaller EPR probe. The more extended fluorescent probe can better sense environmental changes spanning larger distances than the smaller spin label probe. The change of relationship of the amino-terminus relative to another part of the Gα is not due to the charge on the probe, since fluorescence results obtained using a large uncharged probe, Bodipy, linked to selected Hexa I mutants also reported significant changes in fluorescence upon activation. This is in contrast to results obtained using smaller bimane probes, which showed relatively little changes in fluorescence upon activation (Table 2). The fluorescence reflects changes in the global environment of the labeled residue, while EPR reflects changes in the local dynamics of the individually labeled residue. Together these techniques describe the secondary, tertiary, and global environment of the amino-terminus.

If the amino-terminus folds back on the Gα molecule in the activated state, the structure of the amino-terminus may represent a random coil with changes in the hydrophobicity resulting from an increase in proximity of the amino-terminus to other parts of the Gα subunit in the GDP-AlF_4^- bound state, reflecting a global change in environment for the amino-terminus. Interestingly, the residues with the greatest LY fluorescence increase upon activation (K10, V13, K17, R21) localized to a distinct face of the helix near the interface between the G$\beta\gamma$ binding site and solvent exposed amino-terminal residues (Figure 2A). Alignment of these residues among heterotrimeric G protein families reveals conservation of charged, basic residues at positions homologous to 10, 17, and 21. These charged, basic residues are absolutely conserved across all G protein family members at positions 10 and 21, with the exception of position 10 in G_{12} and position 21 in G_{13}. The charged, basic residue at position 17 is absolutely conserved among all G protein family members except that of the G_q family. The electrostatic potential of the Gα subunit's surface reveals a surface rich in acidic residues that provide many potential binding sites for the positively charged amino-terminus in the activated state, while the surface potential rendering of the amino-terminal helix itself reveals both hydrophobic and basic residues which may conceivably play a part in an intramolecular binding event (Figure 3A). This potential intramolecular docking site may explain the fact that myristoylated $G\alpha_t$-GTP is quite soluble, despite its hydrophobic amino-terminal tail, while GDP bound free α subunits tend to oligomerize (*21*). Since GTP-bound Gα subunits dissociate from G$\beta\gamma$ in cells, and since myristoylation is not sufficient to tether soluble Gα-GTP to the membrane (*24*), an intramolecular binding site for the amino-terminus would account for these observations. A precedent for an intramolecular docking site for a myristoylated amino-terminal region is the catalytic subunit of cAMP-dependent protein kinase (*23*).

The G$\beta\gamma$ subunit binding to the Gα amino-terminus may facilitate the formation and the stability of an α-helical structure in this region. The EPR results presented in Figure 4 show clear evidence for a disorder-to-order transition in the Gα-GDP amino-terminal domain upon complex formation with G$\beta\gamma$. The disordered state resembles a random coil. Although it is impossible to assign the structure of the ordered state based on the limited EPR data set, both the side chain dynamics and the sequence-dependence are consistent with a helix as seen in the crystal structure of heterotrimeric G proteins.

The fact that little change is seen in the EPR spectra of any of the labeled mutants in the heterotrimer upon the addition of urea-washed ROS membranes in the dark or after photobleaching suggests that the amino-terminal domain of Gα is not directly involved in interaction with dark or activated rhodopsin. To strengthen this conclusion, quantitative binding of the labeled heterotrimer to dark and photobleached ROS membranes must be demonstrated. However, the data in Figure 5 show that productive interaction of the labeled heterotrimer does occur with light-activated rhodopsin, and that GTPγS stimulated release of the Gα-GTPγS subunit does occur. In the Gα-GTPγS state, the amino-terminal domain is again disordered, closely resembling the Gα-GDP state. It is important to recognize that the spin labeled probe is similar in size to the smaller, more compact fluorescent probes which registered very little changes upon activation (Table 2, Figure 2D); these more compact probes are consequently less sensitive reporters of longer range interactions than larger, more extended fluorescent probes.

Some studies suggest that the amino-terminus of Gα subunits may participate in forming the binding site for cognate receptors (*10, 11*). Other studies also implicate Gα amino-terminus in receptor activation (*22*). Recently, a turn was removed from the amino-terminal helix of a $G\alpha_s$-like chimera to determine if receptor activation results in a tilt of G$\beta\gamma$ relative to Gα, thus easing nucleotide release (*12*). By coexpressing this $G\alpha_s$ chimera with G$\beta\gamma$ and measuring cAMP activation, Bourne et al. (*12*) found that G$\beta\gamma$ is required for optimal activation of this $G\alpha_s$ chimera. Although not direct proof, their results suggest there may be a critical role for the amino-terminus of Gα in receptor-mediated activation of Gα subunits. Our results have not demonstrated any striking receptor-mediated changes in the conformation of the amino-terminus upon light activation (Figure 5).

Additionally, an influence of the acyl group on amino-terminal conformation in the native, posttranslationally modified protein cannot be ruled out, since conformational changes may result from cooperative binding of G$\beta\gamma$ and membrane components. A comparison of the behavior of myristoylated and nonmyristoylated Cys mutant would illuminate the role of myristoylation in amino-terminal conformational changes.

It should be noted that the series of EPR experiments shown in Figure 5 leading to release of the activated Gα subunit can be carried out with only 5 nmol of labeled G$\alpha\beta\gamma$, and can be followed in time with a resolution of milliseconds. Thus, use of spin-labeled Gα can be used as the basis of a rapid quantitative assay for receptor activation of G proteins.

In summary, the amino-terminus changes conformation in the G protein cycle, as evidenced by fluorescence and EPR changes upon G$\beta\gamma$ binding and activation to either the GDP-AlF_4^- transition state or the GTPγS bound conformation. Using reporters all along the amino-terminus, these results paint a picture of a dynamic amino-terminal region in the native protein in solution. The challenge will be to define these changes and their effects on the G-protein cycle. Further EPR and fluorescence studies of these mutants as well as

their myristoylated counterparts in conjunction with G$\beta\gamma$ and activated receptor will extend our knowledge regarding the role of the amino-terminus of Gα in membrane binding, receptor interaction, and G-protein activation.

ACKNOWLEDGMENT

We thank Maurine Linder for the $G\alpha_{i1}$ expression vector.

REFERENCES

1. Lambright, D. G., Sondek, J., Bohm, A., Skiba, N. P., Hamm, H. E., and Sigler, P. B. (1996) The 2.0 Å crystal structure of a heterotrimeric G protein. *Nature 379*, 311−319.
2. Wall, M. A., Coleman, D. E., Lee, E., Iniguez-Lluhi, J. A., Posner, B. A., Gilman, A. G., and Sprang, S. R. (1995) The structure of the G protein heterotrimer $G_{i\alpha1}\beta_1\gamma_2$. *Cell 83*, 1047−1058.
3. Mixon, M. B., Lee, E., Coleman, D. E., Berghuis, A. M., Gilman, A. G., and Sprang, S. R. (1995) Tertiary and quaternary structural changes in $G_{i\alpha1}$ induced by GTP hydrolysis. *Science 270*, 954−960.
4. Coleman, D. E., Berghuis, A. M., Lee, E., Linder, M. E., Gilman, A. G., and Sprang, S. R. (1994) Structures of active conformations of $G_{i\alpha1}$ and the mechanism of GTP hydrolysis. *Science 265*, 1405−1412.
5. Lambright, D. G., Noel, J. P., Hamm, H. E., and Sigler, P. B. (1994) Structural determinants for activation of the α-subunit of a heterotrimeric G protein. *Nature 369*, 621−628.
6. Noel, J. P., Hamm, H. E., and Sigler, P. B. (1993) The 2. 2 Å crystal structure of transducin-α complexed with GTPγS. *Nature 366*, 654−663.
7. Mazzoni, M. R., Malinski, J. A., and Hamm, H. E. (1991) Structural analysis of rod GTP-binding protein, G_t. Limited proteolytic digestion pattern of G_t with four proteases defines monoclonal antibody epitope. *J. Biol. Chem. 266*, 14072−14081.
8. Bradford, M. M. (1976) A rapid and sensitive method for the quantitation of microgram quantities of protein utilizing the principle of protein-dye binding. *Anal. Biochem. 72*, 248−254.
9. Yang, C. S., Skiba, N. P., Mazzoni, M. R., and Hamm, H. E. (1999) Conformational changes at the carboxyl terminus of Gα occur during G protein activation. *J. Biol. Chem. 274*, 2379−2385.
10. Hamm, H. E., Deretic, D., Arendt, A., Hargrave, P. A., Koenig, B., and Hofmann, K. P. (1988) Site of G protein binding to rhodopsin mapped with synthetic peptides from the alpha subunit. *Science 241*, 832−835.
11. Kostenis, E., Degtyarev, M. Y., Conklin, B. R., and Wess, J. (1997) The N-terminal extension of $G\alpha_q$ is critical for constraining the selectivity of receptor coupling. *J. Biol. Chem. 272*, 19107−19110.
12. Rondard, P., Iiri, T., Srinivasan, S., Meng, E., Fujita, T., and Bourne, H. R. (2001) Mutant G protein α subunit activated by G$\beta\gamma$: a model for receptor activation? *Proc. Natl. Acad. Sci. U.S.A. 98*, 6150−6155.
13. Langen, R., Cai, K., Altenbach, C., Khorana, H. G. and Hubbell, W. L. (1999) Structural features of the C-terminal domain of bovine rhodopsin: a site-directed spin-labeling study. *Biochemistry 38*, 7918−7924.
14. Klug, C. S., and Feix, J. B. (1998) Guanidine hydrochloride unfolding of a transmembrane beta-strand in FepA using site-directed spin labeling. *Protein Sci. 7*, 1469−1476.
15. Budil, D. E., Lee, S., Saxena, S., and Freed, J. H. (1996) *J. Magn. Reson., Ser. A 120*, (2) 155−189.
16. Columbus, L., Kalai, T., Jeko, J., Hideg, K., and Hubbell, W. L. (2001) Molecular motion of spin labeled side chains in alpha-helices: analysis by variation of side chain structure. *Biochemistry 40*, 3828−3846.
17. Kohnken, R. E., and Hildebrandt, J. D. (1989) G protein subunit interactions. Studies with biotinylated G protein subunits. *J. Biol. Chem. 264*, 20688−20696.
18. Sarvazyan, N. A., Remmers, A. E., and Neubig, R. R. (1998) Determinants of $G_{i1}\alpha$ and $\beta\gamma$ binding. *J. Biol. Chem. 273*, 7394−7940.
19. Skiba, N. P., Bae, H., and Hamm, H. E. (1996) Mapping of effector binding sites of transducin α-subunit using $G\alpha_t/G\alpha_{il}$ chimeras. *J. Biol. Chem. 271*, 413−424.
20. Wang, J., Frost, J. A., Cobb, M. H., and Ross, E. M. (1999) Reciprocal signaling between heterotrimeric G proteins and the p21-stimulated protein kinase. *J. Biol. Chem. 274*, 31641−31647.
21. Mazzoni, M. R., and Hamm, H. E. (1989) Effect of monoclonal antibody binding on α-$\beta\gamma$ subunit interactions in the rod outer segment G protein, Gt. *Biochemistry 28*, 9873−9880.
22. Itoh, Y., Cai, K., and Khorana, H. G. (2001) Mapping of contact sites in complex formation between light activated rhodopsin and transducin by covalent cross-linking: use of a chemically pre-activated reagent. *Proc. Natl. Acad. Sci. U.S.A. 98*, 4883−4887.
23. Zheng, J., Knighton, D. R., Xuong, N. H., Taylor, S. S., Sowadski, J. M., and Ten Eyck, L. F. (1993) Crystal structures of the myristylated catalytic subunit of cAMP-dependent protein kinase reveal open and closed conformations. *Protein Sci. 2*, 1559−1573.
24. Wedegaertner, P. B., Bourne, H. R., and von Zastrom, M. (1996) Activation-induced subcellular redistribution of $G_s\alpha$. *Mol. Biol. Cell 7*, 1225−1233.

BI0255726